Faraday Discussions

SUPPLEMENTARY INFORMATION

A Kinetic Model for Redox-Active Film Based Biophotoelectrodes

D. Buesen,[a] T. Hoefer,[a] H. Zhang,[a] and N. Plumeré,[a*]

Contents

[a]*Center for Electrochemical Sciences (CES), Faculty of Chemistry and Biochemistry, Ruhr University Bochum, Universitätsstr. 150, D-44780 Bochum, Germany. E-mail: nicolas.plumere@rub.de*

1 Conversion Factors for Dimensionless Current

The total current is the sum of the catalytic and the SC2 contributions, which have different conversion factors from the respective dimensionless currents, as shown in equations 1 and 2. Therefore, for the calculation of the total dimensionless current, the dimensionless catalytic and SC2 currents are separately converted to dimensional current before addition.

$$i_{cat} = \iota_{cat} \cdot \left[\frac{l_1}{z_M F A D_M M_{Tot}} \right] \tag{1}$$

$$i_{SC2} = \iota_{SC2} \cdot \left[\frac{l_1}{z_Y F A D_Y Y_{Tot}} \right] \tag{2}$$

For consistency with the reaction stoichiometry, the number of electrons transferred at the electrode surface (z_i) by the mediator and by substrate Y must correspond to the number of electrons transferred in the reactions (ν_i), as shown in equations 3 and 4 for the mediator and for substrate Y respectively.

$$z_M = \nu_Y \tag{3}$$

$$z_Y = \nu_M \tag{4}$$

2 Treatment of Unequal Time Domains

The factor τ_{tot} accounts for the possibility of unequal time durations for the three sections that make up the total time. Since t_{exp} is the primary time-related variable of interest, t_{eq} and t_{rec} are both expressed as multiples of t_{exp}, which are defined respectively as τ_{eq} and τ_{rec} in equations 5 and 6.

$$\tau_{eq} = \frac{t_{eq}}{t_{exp}} \tag{5}$$

$$\tau_{\mathrm{rec}} = \frac{t_{\mathrm{rec}}}{t_{\mathrm{exp}}} \tag{6}$$

Time is scaled with respect to total time, as shown in equation 7 in which unscaled (dimensional) time is denoted with a tilde.

$$t = \frac{\widetilde{t}}{t_{\mathrm{tot}}} = \frac{\widetilde{t}}{t_{\mathrm{exp}}(1+\tau_{\mathrm{eq}}+\tau_{\mathrm{rec}})} = \frac{\widetilde{t}}{t_{\mathrm{exp}}\tau_{\mathrm{tot}}} \tag{7}$$

3 Dimensionless Groups

A concise summary of the basic ω, κ, and σ type groups are contained in tables 1, 2, 3, 4, 5 and 6, with an emphasis on how the variables can be arranged to show either rate ratios of competing processes, or ratios of the diffusion or reaction layer to the film thickness.

Table 1 Summary of ω type dimensionless groups

Mathematical Expression	Units	Physical Description
$\omega_{\mathrm{M}} = \frac{[(l_1)^2/D_{\mathrm{M}}]}{t_{\mathrm{exp}}};\ \omega_{\mathrm{Y}} = \frac{[(l_1)^2/D_{\mathrm{Y}}]}{t_{\mathrm{exp}}};\ \omega_{\mathrm{Z}} = \frac{[(l_1)^2/D_{\mathrm{Z}}]}{t_{\mathrm{exp}}}$	$\frac{\mathrm{s}}{\mathrm{s}}$	$\frac{\text{Time Required to Saturate a Film of Basis Area } (l_1)^2 \text{ by Diffusion}}{\text{Experimental Time}}$
$\omega_{\mathrm{M}}^{-1/2} = \frac{\sqrt{D_{\mathrm{M}} t_{\mathrm{exp}}}}{l_1};\ \omega_{\mathrm{Y}}^{-1/2} = \frac{\sqrt{D_{\mathrm{Y}} t_{\mathrm{exp}}}}{l_1};\ \omega_{\mathrm{Z}}^{-1/2} = \frac{\sqrt{D_{\mathrm{Z}} t_{\mathrm{exp}}}}{l_1}$	$\frac{\mathrm{cm}}{\mathrm{cm}}$	$\frac{\text{Diffusion Layer Thickness of } M, Y, \text{ or } Z}{\text{Film Thickness}}$

Table 2 Summary of enzymatic catalysis related dimensionless groups

Mathematical Expression	Units	Physical Description
$\kappa_{\mathrm{cat}}^{\mathrm{M}} = \frac{k_{\mathrm{cat}} P_{\mathrm{Tot}}}{[(D_{\mathrm{M}} M_{\mathrm{Tot}})/(l_1)^2]};\ \kappa_{\mathrm{cat}}^{\mathrm{Y}} = \frac{k_{\mathrm{cat}} P_{\mathrm{Tot}}}{[(D_{\mathrm{Y}} Y_{\mathrm{Tot}})/(l_1)^2]}$	$\frac{\mathrm{mol{\cdot}cm^{-3}{\cdot}s^{-1}}}{\mathrm{mol{\cdot}cm^{-3}{\cdot}s^{-1}}}$	$\frac{\text{Maximum Enzymatic Catalysis Rate}}{\text{Molar Diffusion Rate of } M \text{ or } Y}$
$\left(\kappa_{\mathrm{cat}}^{\mathrm{M}}\right)^{-1/2} = \frac{\sqrt{D_{\mathrm{M}}[k_{\mathrm{cat}}(P_{\mathrm{Tot}}/M_{\mathrm{Tot}})]^{-1}}}{l_1};\ \left(\kappa_{\mathrm{cat}}^{\mathrm{Y}}\right)^{-1/2} = \frac{\sqrt{D_{\mathrm{Y}}[k_{\mathrm{cat}}(P_{\mathrm{Tot}}/Y_{\mathrm{Tot}})]^{-1}}}{l_1}$	$\frac{\mathrm{cm}}{\mathrm{cm}}$	$\frac{M \text{ or } Y \text{ Reaction Layer Thickness}}{\text{Film Thickness}}$
$\theta_{\mathrm{MM}} = \frac{k_{\mathrm{cat}} P_{\mathrm{Tot}}}{k_{\mathrm{PY}} M_{\mathrm{Tot}} P_{\mathrm{Tot}}}$	$\frac{\mathrm{mol{\cdot}cm^{-3}{\cdot}s^{-1}}}{\mathrm{mol{\cdot}cm^{-3}{\cdot}s^{-1}}}$	$\frac{\text{Maximum Enzymatic Catalysis Rate}}{\text{Maximum Electron Transfer Rate}}$
$\mu = \frac{K_{\mathrm{M}}}{Y_{\mathrm{Tot}}}$	$\frac{\mathrm{mol{\cdot}cm^{-3}}}{\mathrm{mol{\cdot}cm^{-3}}}$	$\frac{\text{Enzyme Saturation Concentration}}{\text{Substrate Concentration}}$

Table 3 Summary of bimolecular catalysis related dimensionless groups

Mathematical Expression	Units	Physical Description
$\kappa_{\mathrm{PY}}^{\mathrm{M}} = \frac{k_{\mathrm{PY}} P_{\mathrm{Tot}} Y_{\mathrm{Tot}}}{[D_{\mathrm{M}} M_{\mathrm{Tot}}/(l_1)^2]};\ \kappa_{\mathrm{PY}}^{\mathrm{Y}} = \frac{k_{\mathrm{PY}} P_{\mathrm{Tot}} Y_{\mathrm{Tot}}}{[D_{\mathrm{Y}} Y_{\mathrm{Tot}}/(l_1)^2]}$	$\frac{\mathrm{mol{\cdot}cm^{-3}{\cdot}s^{-1}}}{\mathrm{mol{\cdot}cm^{-3}{\cdot}s^{-1}}}$	$\frac{\text{Maximum Bimolecular Catalysis Rate}}{\text{Molar Diffusion Rate of } M \text{ or } Y}$
$\left(\kappa_{\mathrm{PY}}^{\mathrm{M}}\right)^{-1/2} = \frac{\sqrt{D_{\mathrm{M}}[k_{\mathrm{PY}} P_{\mathrm{Tot}}(Y_{\mathrm{Tot}}/M_{\mathrm{Tot}})]^{-1}}}{l_1};\ \left(\kappa_{\mathrm{PY}}^{\mathrm{Y}}\right)^{-1/2} = \frac{\sqrt{D_{\mathrm{Y}}[k_{\mathrm{PY}} P_{\mathrm{Tot}}(M_{\mathrm{Tot}}/Y_{\mathrm{Tot}})]^{-1}}}{l_1}$	$\frac{\mathrm{cm}}{\mathrm{cm}}$	$\frac{M \text{ or } Y \text{ Reaction Layer Thickness}}{\text{Film Thickness}}$
$\theta_{\mathrm{MP}} = \frac{k_{\mathrm{PY}} Y_{\mathrm{Tot}} P_{\mathrm{Tot}}}{k_{\mathrm{MP}} M_{\mathrm{Tot}} P_{\mathrm{Tot}}}$	$\frac{\mathrm{mol{\cdot}cm^{-3}{\cdot}s^{-1}}}{\mathrm{mol{\cdot}cm^{-3}{\cdot}s^{-1}}}$	$\frac{\text{Maximum Bimolecular Catalysis Rate}}{\text{Maximum Electron Transfer Rate}}$

Table 4 Summary of solar fuel generation related dimensionless groups

Mathematical Expression	Units	Physical Description
$\kappa_{YZ}^{Y} = \frac{k_{YZ} Y_{Tot} Z_{Tot}}{[D_Y Y_{Tot}/(l_1)^2]}$; $\kappa_{YZ}^{Z} = \frac{k_{YZ} Y_{Tot} Z_{Tot}}{[D_Z Z_{Tot}/(l_1)^2]}$	$\frac{mol \cdot cm^{-3} \cdot s^{-1}}{mol \cdot cm^{-3} \cdot s^{-1}}$	$\frac{\text{Maximum Reaction Rate of } Y \text{ With } Z}{\text{Molar Diffusion Rate of } Y \text{ or } Z}$
$\left(\kappa_{YZ}^{Y}\right)^{-1/2} = \frac{\sqrt{D_Y (k_{YZ} Z_{Tot})^{-1}}}{l_1}$; $\left(\kappa_{YZ}^{Z}\right)^{-1/2} = \frac{\sqrt{D_Z (k_{YZ} Y_{Tot})^{-1}}}{l_1}$	$\frac{cm}{cm}$	$\frac{Y \text{ or } Z \text{ Reaction Layer Thickness}}{\text{Film Thickness}}$

Table 5 Summary of SC1 process related dimensionless groups

Mathematical Expression	Units	Physical Description
$\kappa_{SC1}^{Y} = \frac{k_{SC1} M_{Tot} Y_{Tot}}{[D_Y Y_{Tot}/(l_1)^2]}$; $\kappa_{SC1}^{M} = \frac{k_{SC1} Y_{Tot} M_{Tot}}{[D_M M_{Tot}/(l_1)^2]}$	$\frac{mol \cdot cm^{-3} \cdot s^{-1}}{mol \cdot cm^{-3} \cdot s^{-1}}$	$\frac{\text{Maximum Reaction Rate of } Y \text{ With } M}{\text{Molar Diffusion Rate of } Y \text{ or } M}$
$\left(\kappa_{SC1}^{Y}\right)^{-1/2} = \frac{\sqrt{D_Y (k_{SC1} M_{Tot})^{-1}}}{l_1}$; $\left(\kappa_{SC1}^{M}\right)^{-1/2} = \frac{\sqrt{D_M (k_{SC1} Y_{Tot})^{-1}}}{l_1}$	$\frac{cm}{cm}$	$\frac{Y \text{ or } M \text{ Reaction Layer Thickness}}{\text{Film Thickness}}$

Table 6 Summary of σ related dimensionless groups

Mathematical Expression	Units	Physical Description
$\upsilon_M = \frac{k_M^0 M_{Tot}}{(D_M M_{tot}/l_1)}$; $\upsilon_Y = \frac{k_Y^0 Y_{Tot}}{(D_Y Y_{Tot}/l_1)}$	$\frac{mol \cdot cm^{-2} \cdot s^{-1}}{mol \cdot cm^{-2} \cdot s^{-1}}$	$\frac{\text{Electron Transfer Rate of } M \text{ or } Y \text{ at the Electrode Surface}}{\text{Diffusion Speed of a Plane of } M \text{ or } Y \text{ Within the Film}}$
$\varepsilon_M = \frac{(E - E_M^0)}{(RT/n_M F)}$; $\varepsilon_Y = \frac{(E - E_Y^0)}{(RT/n_Y F)}$	$\frac{V}{\nabla}$	$\frac{\text{Overpotential of the System}}{\text{Reference Potential at Temperature } T}$
$\sigma_b^M = \upsilon_M \, exp[\varepsilon_M (1 - \alpha_M)]$; $\sigma_b^Y = \upsilon_Y \, exp[\varepsilon_Y (1 - \alpha_Y)]$	$\frac{mol \cdot cm^{-2} \cdot s^{-1}}{mol \cdot cm^{-2} \cdot s^{-1}}$	$\frac{\text{Oxidation Rate of } M \text{ or } Y \text{ at the Electrode Surface}}{\text{Diffusion Speed of a Plane of } M \text{ or } Y \text{ Within the Film}}$
$\sigma_f^M = \upsilon_M \, exp[-\alpha_M \varepsilon_M]$; $\sigma_f^Y = \upsilon_Y \, exp[-\alpha_Y \varepsilon_Y]$	$\frac{mol \cdot cm^{-2} \cdot s^{-1}}{mol \cdot cm^{-2} \cdot s^{-1}}$	$\frac{\text{Reduction Rate of } M \text{ or } Y \text{ at the Electrode Surface}}{\text{Diffusion Speed of a Plane of } M \text{ or } Y \text{ Within the Film}}$

4 Standalone App for Simulations

In order to facilitate the calculation of dimensionless groups and for running full simulations, a standalone app was developed by the use of Matlab App Designer and Matlab Compiler. Installation of the app automatically installs Matlab Runtime, which allows for programs developed by Matlab to be used in a stand alone setting (i.e. without requiring the purchase of Matlab or other software). After entering the dimensional parameters into the app, simulated current-time curves can be generated as shown in figure 1A. Additionally, concentration profiles at specified times can be obtained, as shown in figure 1B.

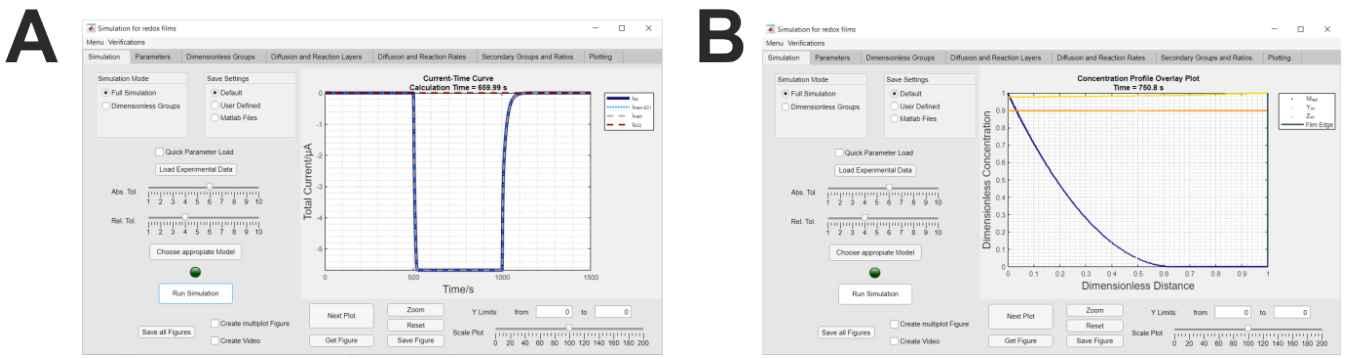

Fig. 1 Screenshot of the app, showing resulting current-time curve (A), and concentration profiles at selected times (B).

The app is also useful for the calculation of reaction rate ratios and for the ratios of the diffusion or reaction layers to the film thickness, which are located in the app under the tabs “Diffusion and Reaction Rates” and “Diffusion and Reaction Layers”; example screenshots of these are shown in the left and right sides of figure 2 respectively. The use of gauges, in which the quantity of interest is expressed in a logarithmic scale provides a visual representation; rate ratios are represented by half-circular gauges, and ratios of diffusion or reaction layers to the film thickness are represented by linear gauges.

Fig. 2 Screenshot of the app, with half circular gauges for rate ratios (A), and linear gauges for ratios of the diffusion or reaction layer to the film thickness (B). Both types of gauges report results on a logarithmic scale.

More details regarding the use of the app will be included in a user manual which will be built into the app and accessible by means of a selection menu.

5 Finite Difference Equations

The finite difference equations presented here are for the most complicated mechanism, and for within the film. Equations for simplified mechanisms, or for the solution domain, can be derived by setting the appropriate quantities to zero.

5.1 Finite Volume Method Schematic

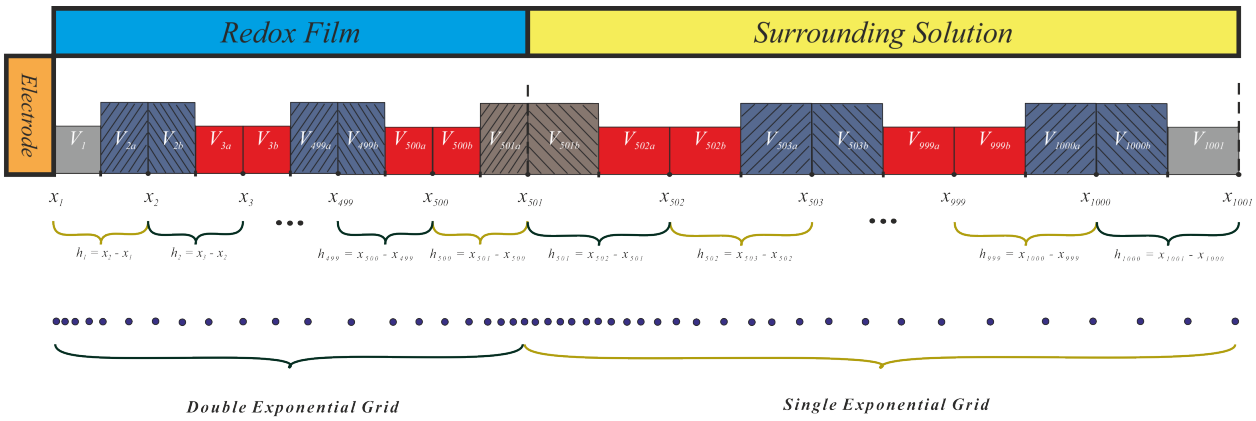

Fig. 3 Finite volume method discretization scheme into 1001 control volumes with a double exponential grid for the film domain and a single exponential grid for the surrounding solution domain.

The finite difference equations were derived based upon guidelines for the finite volume method[1]. A schematic of the finite difference scheme was constructed, and is shown in figure 3. The scheme allows for arbitrary variable spacing between the space points. The number of points is variable, as a multiple of 250 per space domain (i.e. a multiple of 1 results in 250 points for each of the two space domains for a total of 500 space points). For clarity, the example of 1000 total points (1001 finite volumes) is given in this section. In this scheme, the spatial discontinuity (film/solution interface) is located at the center of one of the finite volume elements.

In order to optimize efficiency with regards to the number of spatial points, the spatial points were concentrated in the areas where demands on the system are higher due to rapidly changing concentration profiles (i.e. at the electrode surface, and at the film/surrounding solution interface). Therefore, a "double exponential" grid was constructed for the film domain, where the degree of spacing exponentially increases from the electrode surface to the center of the film, where it begins to exponentially decrease more and more until reaching the film/solution interface, according to a tuning parameter (β_1); higher β_1 values correspond to greater concentration of points at the edges, and a value of zero corresponds to a uniform grid. For the surrounding solution domain, the demands on the system are highest at the film/solution interface and decrease as the concentration profile approaches its bulk value. Therefore, a "single exponential" grid was constructed for the solution domain, in which the spacing exponentially increases from the film/solution interface according to a tuning parameter (β_2). Trends for increasing β_2 are the same as those for β_1; a zero value of β_2 corresponds to a uniform grid, and increasing β_2 values result in greater concentration at the film/solution interface.

5.2 Finite Difference Equations for the Reduced Form of the Mediator (M_{red})

5.2.1 At the Electrode

For i = 1

$$\left(\frac{\partial M_{red}}{\partial t}\right)_{x_i} = \left(\frac{2}{h_i}\right)\left(\frac{\tau_{tot}}{\omega_M}\right)\{A - B - C + D\} \tag{8}$$

$$\mathrm{A} = \frac{1}{(1+\zeta_{\mathrm{x}})^2}\left[\frac{(M_{\mathrm{red}})_{\mathrm{x_{i+1}}} - (M_{\mathrm{red}})_{\mathrm{x_i}}}{h_{\mathrm{i}}}\right] - \frac{1}{(1+\zeta_{\mathrm{x}})}\left[\sigma_{\mathrm{b}}^{\mathrm{M}}(M_{\mathrm{red}}) - \sigma_{\mathrm{f}}^{\mathrm{M}}(1-M_{\mathrm{red}})_{\mathrm{x_i}}\right] \tag{9}$$

$$\mathrm{B} = \frac{(\nu_{\mathrm{M}})\,\kappa_{\mathrm{cat}}^{\mathrm{M}}\,(M_{\mathrm{red}})_{\mathrm{x_i}}\,(Y_{\mathrm{ox}})_{\mathrm{x_i}}}{\left(\frac{1}{\nu_{\mathrm{M}}}\right)\mu\,(M_{\mathrm{red}})_{\mathrm{x_i}} + \left(\frac{1}{\nu_{\mathrm{M}}}\right)(M_{\mathrm{red}})_{\mathrm{x_i}}\,(Y_{\mathrm{ox}})_{\mathrm{x_i}} + \vartheta_{\mathrm{MM}}\,(Y_{\mathrm{ox}})_{\mathrm{x_i}}}\left(\frac{h_{\mathrm{i}}}{2}\right) \tag{10}$$

$$\mathrm{C} = \frac{(\nu_{\mathrm{M}})\,\kappa_{\mathrm{PY}}^{\mathrm{M}}\,(M_{\mathrm{red}})_{\mathrm{x_i}}\,(Y_{\mathrm{ox}})_{\mathrm{x_i}}}{\left(\frac{1}{\nu_{\mathrm{M}}}\right)(M_{\mathrm{red}})_{\mathrm{x_i}} + \vartheta_{\mathrm{MP}}\,(Y_{\mathrm{ox}})_{\mathrm{x_i}}}\left(\frac{h_{\mathrm{i}}}{2}\right) \tag{11}$$

$$\mathrm{D} = \left(\frac{\nu_{\mathrm{M}}}{\nu_{\mathrm{Y}}}\right)\kappa_{\mathrm{SC1}}^{\mathrm{M}}\left[(1-(M_{\mathrm{red}})_{\mathrm{x_i}}\right]\left[(1-(Y_{\mathrm{ox}})_{\mathrm{x_i}}\right]\left(\frac{h_{\mathrm{i}}}{2}\right) \tag{12}$$

5.2.2 Within the Film

For $\mathrm{i} = 2-500$

$$\left(\frac{\partial M_{\mathrm{red}}}{\partial t}\right)_{\mathrm{x_i}} = \left(\frac{2}{h_{\mathrm{i-1}}+h_{\mathrm{i}}}\right)\left(\frac{\tau_{\mathrm{tot}}}{\omega_{\mathrm{M}}}\right)\{\mathrm{A}-\mathrm{B}-\mathrm{C}+\mathrm{D}\} \tag{13}$$

$$\mathrm{A} = \frac{1}{(1+\zeta_{\mathrm{x}})^2}\left[\frac{(M_{\mathrm{red}})_{\mathrm{x_{i+1}}} - (M_{\mathrm{red}})_{\mathrm{x_i}}}{h_{\mathrm{i}}}\right] - \frac{1}{(1+\zeta_{\mathrm{x}})^2}\left[\frac{(M_{\mathrm{red}})_{\mathrm{x_i}} - (M_{\mathrm{red}})_{\mathrm{x_{i-1}}}}{h_{\mathrm{i-1}}}\right] \tag{14}$$

$$\mathrm{B} = \frac{(\nu_{\mathrm{M}})\,\kappa_{\mathrm{cat}}^{\mathrm{M}}\,(M_{\mathrm{red}})_{\mathrm{x_i}}\,(Y_{\mathrm{ox}})_{\mathrm{x_i}}}{\left(\frac{1}{\nu_{M}}\right)\mu\,(M_{\mathrm{red}})_{\mathrm{x_i}} + \left(\frac{1}{\nu_{M}}\right)(M_{\mathrm{red}})_{\mathrm{x_i}}\,(Y_{\mathrm{ox}})_{\mathrm{x_i}} + \vartheta_{\mathrm{MM}}\,(Y_{\mathrm{ox}})_{\mathrm{x_i}}}\left(\frac{h_{\mathrm{i-1}}+h_{\mathrm{i}}}{2}\right) \tag{15}$$

$$\mathrm{C} = \frac{(\nu_{\mathrm{M}})\,\kappa_{\mathrm{PY}}^{\mathrm{M}}\,(M_{\mathrm{red}})_{\mathrm{x_i}}\,(Y_{\mathrm{ox}})_{\mathrm{x_i}}}{\left(\frac{1}{\nu_{\mathrm{M}}}\right)(M_{\mathrm{red}})_{\mathrm{x_i}} + \vartheta_{\mathrm{MP}}\,(Y_{\mathrm{ox}})_{\mathrm{x_i}}}\left(\frac{h_{\mathrm{i-1}}+h_{\mathrm{i}}}{2}\right) \tag{16}$$

$$\mathrm{D} = \left(\frac{\nu_{\mathrm{M}}}{\nu_{\mathrm{Y}}}\right)\kappa_{\mathrm{SC1}}^{\mathrm{M}}\left[(1-(M_{\mathrm{red}})_{\mathrm{x_i}}\right]\left[(1-(Y_{\mathrm{ox}})_{\mathrm{x_i}}\right]\left(\frac{h_{\mathrm{i-1}}+h_{\mathrm{i}}}{2}\right) \tag{17}$$

5.2.3 At the Film/Solution Interface

For $\mathrm{i} = 501$

$$\left(\frac{\partial M_{\mathrm{red}}}{\partial t}\right)_{\mathrm{x_i}} = \left(\frac{2}{h_{\mathrm{i-1}}}\right)\left(\frac{\tau_{\mathrm{tot}}}{\omega_{\mathrm{M}}}\right)\{\mathrm{A}-\mathrm{B}-\mathrm{C}+\mathrm{D}\} \tag{18}$$

$$\mathrm{A} = -\frac{1}{(1+\zeta_{\mathrm{x}})^2}\left[\frac{(M_{\mathrm{red}})_{\mathrm{x_i}} - (M_{\mathrm{red}})_{\mathrm{x_{i-1}}}}{h_{\mathrm{i-1}}}\right] \tag{19}$$

$$\mathrm{B} = \frac{(\nu_{\mathrm{M}})\,\kappa_{\mathrm{cat}}^{\mathrm{M}}\,(M_{\mathrm{red}})_{\mathrm{x_i}}\,(Y_{\mathrm{ox}})_{\mathrm{x_i}}}{\left(\frac{1}{\nu_{\mathrm{M}}}\right)\mu\,(M_{\mathrm{red}})_{\mathrm{x_i}} + \left(\frac{1}{\nu_{\mathrm{M}}}\right)(M_{\mathrm{red}})_{\mathrm{x_i}}\,(Y_{\mathrm{ox}})_{\mathrm{x_i}} + \vartheta_{\mathrm{MM}}\,(Y_{\mathrm{ox}})_{\mathrm{x_i}}}\left(\frac{h_{\mathrm{i-1}}}{2}\right) \tag{20}$$

$$\mathrm{C} = \frac{(\nu_{\mathrm{M}})\,\kappa_{\mathrm{PY}}^{\mathrm{M}}\,(M_{\mathrm{red}})_{\mathrm{x_i}}\,(Y_{\mathrm{ox}})_{\mathrm{x_i}}}{\left(\frac{1}{\nu_{\mathrm{M}}}\right)(M_{\mathrm{red}})_{\mathrm{x_i}} + \vartheta_{\mathrm{MP}}\,(Y_{\mathrm{ox}})_{\mathrm{x_i}}}\left(\frac{h_{\mathrm{i-1}}}{2}\right) \tag{21}$$

$$\mathrm{D} = \left(\frac{\nu_{\mathrm{M}}}{\nu_{\mathrm{Y}}}\right)\kappa_{\mathrm{SC1}}^{\mathrm{M}}\left[(1-(M_{\mathrm{red}})_{\mathrm{x_i}}\right]\left[(1-(Y_{\mathrm{ox}})_{\mathrm{x_i}}\right]\left(\frac{h_{\mathrm{i-1}}}{2}\right) \tag{22}$$

5.2.4 In the Surrounding Solution

For $\mathrm{i} = 502 - 1000$

$$\left(\frac{\partial M_{\mathrm{red}}}{\partial t}\right)_{\mathrm{x_i}} = 0 \tag{23}$$

The application of equation 23 will hold $(M_{\mathrm{red}})_{\mathrm{x_i}}$ at its initial value (zero in this case).

5.2.5 At the Bulk

For $\mathrm{i} = 1001$

$$\left(\frac{\partial M_{\mathrm{red}}}{\partial t}\right)_{\mathrm{x_i}} = 0 \tag{24}$$

The application of equation 24 will hold $(M_{\mathrm{red}})_{\mathrm{x_i}}$ at its initial value (zero in this case).

5.3 Finite Difference Equations for the Oxidized Form of Electron Acceptor Y

5.3.1 At the Electrode

For $\mathrm{i} = 1$

$$\left(\frac{\partial Y_{\mathrm{ox}}}{\partial t}\right)_{\mathrm{x_i}} = \left(\frac{2}{h_{\mathrm{i}}}\right)\left(\frac{\tau_{\mathrm{tot}}}{\omega_{\mathrm{Y}}}\right)\{\mathrm{A} - \mathrm{B} - \mathrm{C} + \mathrm{D} + \mathrm{E}\} \tag{25}$$

$$\mathrm{A} = \frac{1}{(1+\zeta_{\mathrm{x}})^2}\left[\frac{(Y_{\mathrm{ox}})_{\mathrm{x_{i+1}}} - (Y_{\mathrm{ox}})_{x_{\mathrm{i}}}}{h_{\mathrm{i}}}\right] - \frac{1}{(1+\zeta_{\mathrm{x}})}\left[\sigma_{\mathrm{f}}^{\mathrm{Y}}\,(Y_{\mathrm{ox}})_{\mathrm{x_i}} - \sigma_{\mathrm{b}}^{\mathrm{Y}}(1 - Y_{\mathrm{ox}})\right] \tag{26}$$

$$\mathrm{B} = \frac{\left(\frac{1}{\nu_M}\right)\kappa_{\mathrm{cat}}^{\mathrm{Y}}\,(M_{\mathrm{red}})_{\mathrm{x_i}}\,(Y_{\mathrm{ox}})_{\mathrm{x_i}}}{\left(\frac{1}{\nu_M}\right)\mu\,(M_{\mathrm{red}})_{\mathrm{x_i}} + \left(\frac{1}{\nu_M}\right)(M_{\mathrm{red}})_{\mathrm{x_i}}\,(Y_{\mathrm{ox}})_{\mathrm{x_i}} + \vartheta_{\mathrm{MM}}\,(Y_{\mathrm{ox}})_{\mathrm{x_i}}}\left(\frac{h_{\mathrm{i}}}{2}\right) \tag{27}$$

$$\mathrm{C} = \frac{\left(\frac{1}{\nu_{\mathrm{M}}}\right)\kappa_{\mathrm{PY}}^{\mathrm{Y}}\,(M_{\mathrm{red}})_{\mathrm{x_i}}\,(Y_{\mathrm{ox}})_{\mathrm{x_i}}}{\left(\frac{1}{\nu_{\mathrm{M}}}\right)(\vartheta_{\mathrm{MP}})^{-1}\,(M_{\mathrm{red}})_{\mathrm{x_i}} + (Y_{\mathrm{ox}})_{\mathrm{x_i}}}\left(\frac{h_{\mathrm{i}}}{2}\right) \tag{28}$$

$$\mathrm{D} = \left(\frac{\nu_{\mathrm{Y}}}{\nu_{\mathrm{M}}}\right)\kappa_{\mathrm{SC1}}^{\mathrm{Y}}\left[(1 - (M_{\mathrm{red}})_{\mathrm{x_i}}\right]\left[(1 - (Y_{\mathrm{ox}})_{\mathrm{x_i}}\right]\left(\frac{h_{\mathrm{i}}}{2}\right) \tag{29}$$

$$\mathrm{E} = \kappa_{\mathrm{YZ}}^{\mathrm{Y}}\,(Z_{\mathrm{ox}})_{\mathrm{x_i}}\left[(1 - (Y_{\mathrm{ox}})_{\mathrm{x_i}}\right]\left(\frac{h_{\mathrm{i}}}{2}\right) \tag{30}$$

5.3.2 Within the Film

For $\mathrm{i} = 2 - 500$

$$\left(\frac{\partial Y_{\mathrm{ox}}}{\partial t}\right)_{\mathrm{x_i}} = \left(\frac{2}{h_{\mathrm{i-1}}+h_{\mathrm{i}}}\right)\left(\frac{\tau_{\mathrm{tot}}}{\omega_{\mathrm{Y}}}\right)\{\mathrm{A}-\mathrm{B}-\mathrm{C}+\mathrm{D}+\mathrm{E}\} \tag{31}$$

$$\mathrm{A} = \frac{1}{(1+\zeta_{\mathrm{x}})^2}\left[\frac{(Y_{\mathrm{ox}})_{\mathrm{x_{i+1}}}-(Y_{\mathrm{ox}})_{\mathrm{x_i}}}{h_{\mathrm{i}}}\right] - \frac{1}{(1+\zeta_{\mathrm{x}})^2}\left[\frac{(Y_{\mathrm{ox}})_{\mathrm{x_i}}-(Y_{\mathrm{ox}})_{\mathrm{x_{i-1}}}}{h_{\mathrm{i-1}}}\right] \tag{32}$$

$$\mathrm{B} = \frac{\left(\frac{1}{\nu_{\mathrm{M}}}\right)\kappa^{\mathrm{Y}}_{\mathrm{cat}}\,(M_{\mathrm{red}})_{\mathrm{x_i}}\,(Y_{\mathrm{ox}})_{\mathrm{x_i}}}{\left(\frac{1}{\nu_{\mathrm{M}}}\right)\mu\,(M_{\mathrm{red}})_{\mathrm{x_i}} + \left(\frac{1}{\nu_{\mathrm{M}}}\right)(M_{\mathrm{red}})_{\mathrm{x_i}}\,(Y_{\mathrm{ox}})_{\mathrm{x_i}} + \vartheta_{\mathrm{MM}}\,(Y_{\mathrm{ox}})_{\mathrm{x_i}}}\left(\frac{h_{\mathrm{i-1}}+h_{\mathrm{i}}}{2}\right) \tag{33}$$

$$\mathrm{C} = \frac{\left(\frac{1}{\nu_{\mathrm{M}}}\right)\kappa^{\mathrm{Y}}_{\mathrm{PY}}\,(M_{\mathrm{red}})_{\mathrm{x_i}}\,(Y_{\mathrm{ox}})_{\mathrm{x_i}}}{\left(\frac{1}{\nu_{\mathrm{M}}}\right)(\vartheta_{\mathrm{MP}})^{-1}\,(M_{\mathrm{red}})_{\mathrm{x_i}} + (Y_{\mathrm{ox}})_{\mathrm{x_i}}}\left(\frac{h_{\mathrm{i-1}}+h_{\mathrm{i}}}{2}\right) \tag{34}$$

$$\mathrm{D} = \left(\frac{\nu_{\mathrm{Y}}}{\nu_{\mathrm{M}}}\right)\kappa^{\mathrm{Y}}_{\mathrm{SC1}}\left[(1-(M_{\mathrm{red}})_{\mathrm{x_i}}\right]\left[(1-(Y_{\mathrm{ox}})_{\mathrm{x_i}}\right]\left(\frac{h_{\mathrm{i-1}}+h_{\mathrm{i}}}{2}\right) \tag{35}$$

$$\mathrm{E} = \kappa^{\mathrm{Y}}_{\mathrm{YZ}}\,(Z_{\mathrm{ox}})_{x_{\mathrm{i}}}\left[(1-(Y_{\mathrm{ox}})_{\mathrm{x_i}}\right]\left(\frac{h_{\mathrm{i-1}}+h_{\mathrm{i}}}{2}\right) \tag{36}$$

5.3.3 At the Film/Solution Interface

For $\mathrm{i} = 501$

$$\left(\frac{\partial Y_{\mathrm{ox}}}{\partial t}\right)_{\mathrm{x_i}} = \left(\frac{2}{h_{\mathrm{i-1}}+h_{\mathrm{i}}}\right)\left(\frac{\tau_{\mathrm{tot}}}{\omega_{\mathrm{Y}}}\right)\{\mathrm{A}-\mathrm{B}-\mathrm{C}+\mathrm{D}+\mathrm{E}\} \tag{37}$$

$$\mathrm{A} = \frac{1}{(1+\zeta_{\mathrm{x}})^2}\left[\frac{(Y_{\mathrm{ox}})_{\mathrm{x_{i+1}}}-(Y_{\mathrm{ox}})_{\mathrm{x_i}}}{h_{\mathrm{i}}}\right] - \frac{1}{(1+\zeta_{\mathrm{x}})^2}\left[\frac{(Y_{\mathrm{ox}})_{\mathrm{x_i}}-(Y_{\mathrm{ox}})_{\mathrm{x_{i-1}}}}{h_{\mathrm{i-1}}}\right] \tag{38}$$

$$\mathrm{B} = \frac{\left(\frac{1}{\nu_{\mathrm{M}}}\right)\kappa^{\mathrm{Y}}_{\mathrm{cat}}\,(M_{\mathrm{red}})_{\mathrm{x_i}}\,(Y_{\mathrm{ox}})_{\mathrm{x_i}}}{\left(\frac{1}{\nu_{\mathrm{M}}}\right)\mu\,(M_{\mathrm{red}})_{\mathrm{x_i}} + \left(\frac{1}{\nu_{\mathrm{M}}}\right)(M_{\mathrm{red}})_{\mathrm{x_i}}\,(Y_{\mathrm{ox}})_{\mathrm{x_i}} + \vartheta_{\mathrm{MM}}\,(Y_{\mathrm{ox}})_{\mathrm{x_i}}}\left(\frac{h_{\mathrm{i-1}}}{2}\right) \tag{39}$$

$$\mathrm{C} = \frac{\left(\frac{1}{\nu_{\mathrm{M}}}\right)\kappa^{\mathrm{Y}}_{\mathrm{PY}}\,(M_{\mathrm{red}})_{\mathrm{x_i}}\,(Y_{\mathrm{ox}})_{\mathrm{x_i}}}{\left(\frac{1}{\nu_{\mathrm{M}}}\right)(\vartheta_{\mathrm{MP}})^{-1}\,(M_{\mathrm{red}})_{\mathrm{x_i}} + (Y_{\mathrm{ox}})_{\mathrm{x_i}}}\left(\frac{h_{\mathrm{i-1}}}{2}\right) \tag{40}$$

$$\mathrm{D} = \left(\frac{\nu_{\mathrm{Y}}}{\nu_{\mathrm{M}}}\right)\kappa^{\mathrm{Y}}_{\mathrm{SC1}}\left[(1-(M_{\mathrm{red}})_{\mathrm{x_i}}\right]\left[(1-(Y_{\mathrm{ox}})_{\mathrm{x_i}}\right]\left(\frac{h_{\mathrm{i-1}}}{2}\right) \tag{41}$$

$$\mathrm{E} = \kappa^{\mathrm{Z}}_{\mathrm{YZ}}\,(Z_{\mathrm{ox}})_{\mathrm{x_i}}\left[(1-(Y_{\mathrm{ox}})_{\mathrm{x_i}}\right]\left(\frac{h_{\mathrm{i-1}}}{2}\right) \tag{42}$$

5.3.4 In the Surrounding Solution

For $\mathrm{i} = 502-1000$

$$\left(\frac{\partial Y_{\mathrm{ox}}}{\partial t}\right)_{\mathrm{x_i}} = \left(\frac{2}{h_{\mathrm{i-1}}+h_{\mathrm{i}}}\right)\left(\frac{\tau_{\mathrm{tot}}}{\omega_{\mathrm{Y}}}\right)\{\mathrm{A}+\mathrm{B}\} \tag{43}$$

$$A = \frac{1}{(1+\zeta_x)^2}\left[\frac{(Y_{ox})_{x_{i+1}} - (Y_{ox})_{x_i}}{h_i}\right] - \frac{1}{(1+\zeta_x)^2}\left[\frac{(Y_{ox})_{x_i} - (Y_{ox})_{x_{i-1}}}{h_{i-1}}\right] \tag{44}$$

$$B = \kappa^{Y}_{YZ}(Z_{ox})_{x_i}\left[(1-(Y_{ox})_{x_i}\right]\left(\frac{h_{i-1}+h_i}{2}\right) \tag{45}$$

5.3.5 At the Bulk

For $i = 1001$

$$\left(\frac{\partial Y_{ox}}{\partial t}\right)_{x_i} = 0 \tag{46}$$

Since $(Y_{ox})_{x_i}$, the application of equation 46 will hold $\left[(Y_{ox})_{x_i}\right]_{t=0} = \left[(Y_{ox})_{x_i}\right]_{t=t_{tot}}$ at its initial value.

5.4 Finite Difference Equations for the Oxidized Form of Electron Acceptor Z

5.4.1 At the Electrode

For $i = 1$

$$\left(\frac{\partial Z_{ox}}{\partial t}\right)_{x_i} = \left(\frac{2}{h_i}\right)\left(\frac{\tau_{tot}}{\omega_Z}\right)\{A+B\} \tag{47}$$

$$A = \frac{1}{(1+\zeta_x)^2}\left[\frac{(Z_{ox})_{x_{i+1}} - (Z_{ox})_{x_i}}{h_i}\right] \tag{48}$$

$$B = \kappa^{Z}_{YZ}(Z_{ox})_{x_i}\left[(1-(Y_{ox})_{x_i}\right]\left(\frac{h_i}{2}\right) \tag{49}$$

5.4.2 Within the Film

For $i = 2-500$

$$\left(\frac{\partial Z_{ox}}{\partial t}\right)_{x_i} = \left(\frac{2}{h_{i-1}+h_i}\right)\left(\frac{\tau_{tot}}{\omega_Z}\right)\{A+B\} \tag{50}$$

$$A = \frac{1}{(1+\zeta_x)^2}\left[\frac{(Z_{ox})_{x_{i+1}} - (Z_{ox})_{x_i}}{h_i}\right] - \frac{1}{(1+\zeta_x)^2}\left[\frac{(Z_{ox})_{x_i} - (Z_{ox})_{x_{i-1}}}{h_{i-1}}\right] \tag{51}$$

$$B = \kappa^{Z}_{YZ}(Z_{ox})_{x_i}\left[(1-(Y_{ox})_{x_i}\right]\left(\frac{h_{i-1}+h_i}{2}\right) \tag{52}$$

5.4.3 At the Film/Solution Interface

For $i = 501$

$$\left(\frac{\partial Z_{\mathrm{ox}}}{\partial t}\right)_{\mathrm{x_i}} = \left(\frac{2}{h_{\mathrm{i-1}}+h_{\mathrm{i}}}\right)\left(\frac{\tau_{\mathrm{tot}}}{\omega_{\mathrm{Z}}}\right)\{\mathrm{A}+\mathrm{B}\} \tag{53}$$

$$\mathrm{A} = \frac{1}{(1+\zeta_{\mathrm{x}})^2}\left[\frac{(Z_{\mathrm{ox}})_{\mathrm{x_{i+1}}}-(Z_{\mathrm{ox}})_{\mathrm{x_i}}}{h_{\mathrm{i}}}\right] - \frac{1}{(1+\zeta_{\mathrm{x}})^2}\left[\frac{(Z_{\mathrm{ox}})_{\mathrm{x_i}}-(Z_{\mathrm{ox}})_{\mathrm{x_{i-1}}}}{h_{\mathrm{i-1}}}\right] \tag{54}$$

$$\mathrm{B} = \kappa^{\mathrm{Z}}_{\mathrm{YZ}}(Z_{\mathrm{ox}})_{\mathrm{x_i}}\left[(1-(Y_{\mathrm{ox}})_{\mathrm{x_i}}\right]\left(\frac{h_{\mathrm{i-1}}+h_{\mathrm{i}}}{2}\right) \tag{55}$$

5.4.4 In the Surrounding Solution

For $\mathrm{i} = 502-1000$

$$\left(\frac{\partial Z_{\mathrm{ox}}}{\partial t}\right)_{\mathrm{x_i}} = \left(\frac{2}{h_{\mathrm{i-1}}+h_{\mathrm{i}}}\right)\left(\frac{\tau_{\mathrm{tot}}}{\omega_{\mathrm{Z}}}\right)\{\mathrm{A}+\mathrm{B}\} \tag{56}$$

$$\mathrm{A} = \frac{1}{(1+\zeta_{\mathrm{x}})^2}\left[\frac{(Z_{\mathrm{ox}})_{\mathrm{x_{i+1}}}-(Z_{\mathrm{ox}})_{\mathrm{x_i}}}{h_{\mathrm{i}}}\right] - \frac{1}{(1+\zeta_{\mathrm{x}})^2}\left[\frac{(Z_{\mathrm{ox}})_{\mathrm{x_i}}-(Z_{\mathrm{ox}})_{\mathrm{x_{i-1}}}}{h_{\mathrm{i-1}}}\right] \tag{57}$$

$$\mathrm{B} = \kappa^{\mathrm{Z}}_{\mathrm{YZ}}(Z_{\mathrm{ox}})_{\mathrm{x_i}}\left[(1-(Y_{\mathrm{ox}})_{\mathrm{x_i}}\right]\left(\frac{h_{\mathrm{i-1}}+h_{\mathrm{i}}}{2}\right) \tag{58}$$

5.4.5 At the Bulk

For $\mathrm{i} = 1001$

$$\left(\frac{\partial Z_{ox}}{\partial t}\right)_{x_i} = 0 \tag{59}$$

Since $\left[(Z_{\mathrm{ox}})_{\mathrm{x_i}}\right]_{\mathrm{t=0}} = \left[(Z_{\mathrm{ox}})_{\mathrm{x_i}}\right]_{\mathrm{t=t_{tot}}}$, the application of equation 59 will hold $(Z_{\mathrm{ox}})_{\mathrm{x_i}}$ at its initial value.

6 Piecewise Verification

6.1 Electron Transfer at the Electrode Surface

The heterogeneous electron transfer portion of the model was verified by reduction of the model to contain either the oxidation of M_{red} or the reduction of Y_{ox}; parameters for these two cases are shown in tables 7 and 8, respectively. Overlay plots showing the results for these two cases are shown in figures 4 and 5 respectively.

6.1.1 Verification of Quasi-Reversible Conditions

The Cottrell equation for a planar macroelectrode, shown in equation 60, was used to verify that the electron transfer rate was not reversible for each given set of dimensional parameters. This was done by calculating the expected current-time curve for reversible electron transfer (dashed grey line), and verifying that it did not overlay with the simulation result (solid blue line).

$$i_{\mathrm{rev}} = \frac{z_{\mathrm{i}} F A C_{\mathrm{i}}^{0} \sqrt{D_{\mathrm{i}}}}{\sqrt{\pi t}} \tag{60}$$

As described in the reference textbook[2], a dimensionless parameter (λ) can be calculated which simultaneously considers the effects of k_{i}^{0}, the diffusion coefficient, as well as the measurement time on the overall electron transfer rate as shown in equation 61. Quasi-reversible conditions correspond to λ in the range $10^{-2\alpha} \leq \lambda \leq 2$.

$$\lambda = \frac{2 k_{\mathrm{i}}^{0} \sqrt{t_{\mathrm{tot}}}}{\sqrt{D_{\mathrm{i}}}} \tag{61}$$

6.1.2 Analytical Expressions for Current-Time Curves With Quasi-Reversible Kinetics

An analytical expression from a reference textbook[2] for quasi-reversible kinetics (shown in equation 62) was used for quantitative verification of the simulation for conditions of quasi-reversible electron transfer. This equation is applicable when the system contains only one species (either oxidized or reduced) at its starting condition. The H value needed for equation 62 is given by equation 63 when the diffusion coefficients of the oxidizing and reducing species are equal.

$$i_{\mathrm{quasi}} = z_{\mathrm{i}} F A k_{\mathrm{f}} C_{\mathrm{i}}^{0} \left[exp\left(\mathrm{H}^{2} t\right) erf\left(\mathrm{H}\sqrt{t}\right) \right] \tag{62}$$

$$\mathrm{H} = \frac{k_{\mathrm{f}} + k_{\mathrm{b}}}{\sqrt{D_{\mathrm{i}}}} \tag{63}$$

6.1.3 Mediator Pair ($M_{\mathrm{red}}|M_{\mathrm{ox}}$) Results

For verification of the mediator electron transfer process at the electrode surface, the starting conditions of the film were set to the fully reduced state, and conditions for oxidation under quasi-reversible conditions were set. The overlay of the current-time curve from the simulation with the calculated current-time curve from equation 62 demonstrates correctness of the verification results for quasi-reversible electron transfer. The concentration profile snapshot, shown in figure 4B, taken at 30 s, shows the expected depletion of the reduced form of the mediator near the electrode surface, as well as confinement of M_{red} to the film.

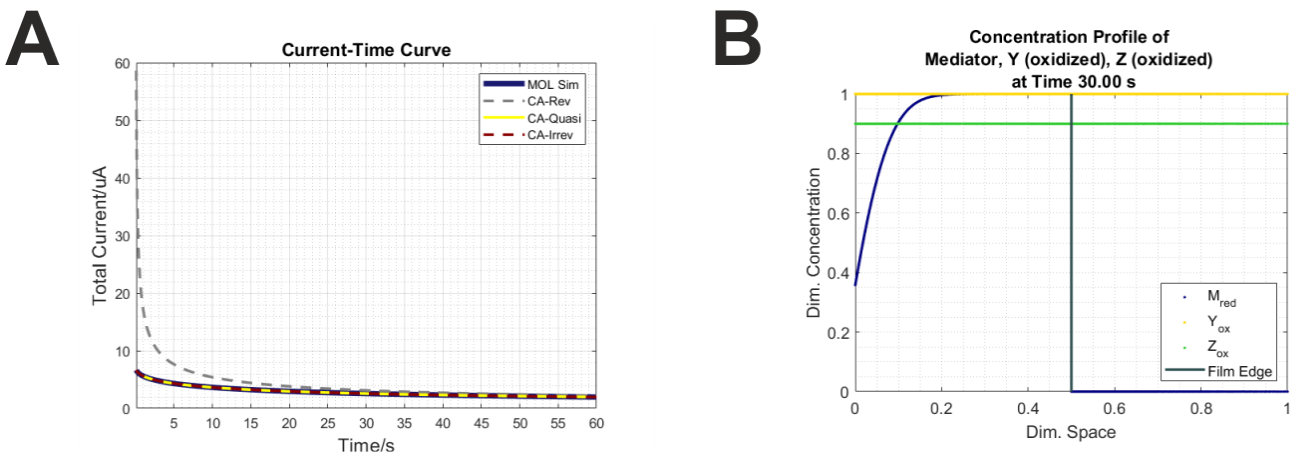

Fig. 4 Mediator electron transfer section verification: overlay of current-time curve with analytical expression for quasi-reversible electron transfer (A), and concentration profile at 30 s (B).

Table 7 Summary of parameters for mediator electron transfer verification

Parameter	Value	Units
M_{tot}	5	mM
M as M_{red}	100	%
k^0_M	1×10^{-5}	$cm\,s^{-1}$
α_M	0.60	Dimensionless
E^0_M	0.800	V
z_M	2	Dimensionless
D_M	1×10^{-6}	$cm^2\,s^{-1}$
l_1	500	μm
ζ_x	1	Dimensionless
d_{el}	2	mm
E	0.900	V
t_{eq}	20	s
t_{exp}	20	s
t_{rec}	20	s
T	20	°C
Space Points	2000	Dimensionless
Time Steps	1000	Dimensionless
β_1	0.01	Dimensionless
β_2	0.01	Dimensionless
Abs Tol	1×10^{-6}	Dimensionless
Rel Tol	1×10^{-4}	Dimensionless

6.1.4 Electron Acceptor Pair ($Y_{red}|Y_{ox}$) Results

For verification of the electron transfer process at the electrode surface for electron acceptor Y, the starting conditions of the system were set to the fully oxidized state, and conditions for reduction under quasi-reversible conditions were set. The overlay of the current-time curve from the simulation with the calculated current-time curve from equation 62 demonstrates correctness of the verification results for quasi-reversible electron transfer. A concentration profile snapshot, shown in figure 5B, shows the expected depletion of the reduced form of the mediator near the electrode surface, as well as the presence of Y_{ox} in both space domains. These calculations also serve as verification of the SC2 portion of the model, since the SC2 process is defined as the oxidation of Y_{red} to Y_{ox} at the electrode surface.

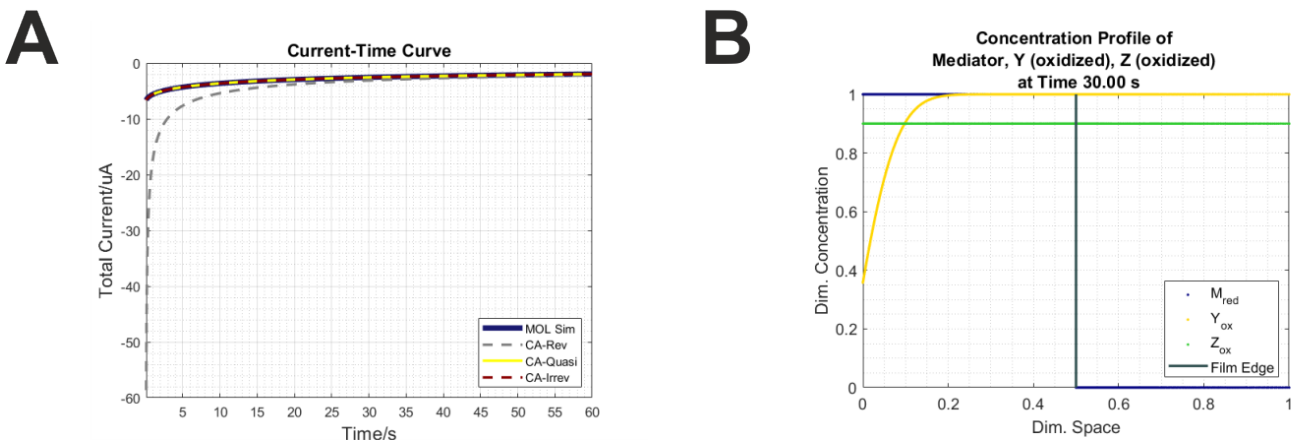

Fig. 5 Results for electron acceptor ($Y_{red}|Y_{ox}$) section verification: overlay of current-time curve with analytical expression for quasi-reversible electron transfer (A), and concentration profile at 30 seconds (B).

Table 8 Summary of parameters for electron acceptor ($Y_{red}|Y_{ox}$) verification

Parameter	Value	Units
Y_{tot}	5	mM
Y as Y_{ox}	100	%
k_Y^0	1×10^{-5}	$cm\,s^{-1}$
α_Y	0.40	Dimensionless
E_Y^0	-0.050	V
z_Y	2	Dimensionless
D_Y	1×10^{-6}	$cm^2\,s^{-1}$
l_1	500	μm
ζ_x	1	Dimensionless
d_{el}	2	mm
E	-0.150	V
t_{eq}	20	s
t_{exp}	20	s
t_{rec}	20	s
T	20	°C
Space Points	2000	Dimensionless
Time Steps	1000	Dimensionless
β_1	0.01	Dimensionless
β_2	0.01	Dimensionless
Abs Tol	1×10^{-6}	Dimensionless
Rel Tol	1×10^{-4}	Dimensionless

6.2 Catalysis Within the Film

6.2.1 Enzymatic Reaction

Successful implementation of the enzymatic catalysis portion of the model was verified by reduction of the model such that the electron transfer and the catalytic (bimolecular) reaction is so fast that only the diffusion of Y limits the system. Since the rightmost (bulk) boundary condition of the surrounding solution space domain sets the concentration to its maximum value (rather than setting the flux equal to zero), setting ζ_x to a small value (0.001) results in a system which corresponds to fast electrode rotation. This allows for direct comparison of the simulation results to those from a reference model[3]. The parameters used are summarized in table 9.

The obtained current-time curve is shown in Figure 6. The steady state concentration profile, taken at 998.5 seconds, is consistent with a region VII assignment, in which M_{red}, but not Y_{ox}, reaches full depletion at a location within the film.

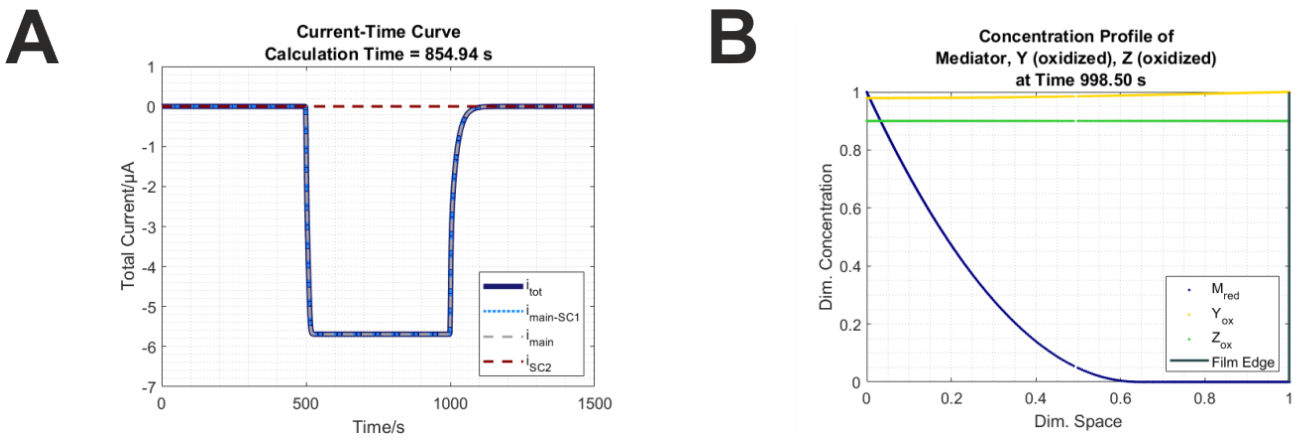

Fig. 6 Enzymatic catalysis section verification. Current-time curve for the main current verification (A), and steady state concentration profile at 998.5 seconds (B).

The analytical expression for the steady state current for a region VII film (Table 3 in the reference article[3]) is shown in equation 64. The calculated value from the analytical expression ($5.70\,\mu$A) closely matches the obtained simulation result.

$$i_{\mathrm{VII}} = z_{\mathrm{M}} F A \sqrt{\frac{2 D_{\mathrm{M}} M_{\mathrm{tot}} k_{\mathrm{cat}} P_{\mathrm{tot}} Y_{\mathrm{tot}}}{K_{\mathrm{M}} + Y_{\mathrm{tot}}}} \tag{64}$$

Table 9 Summary of parameters for enzymatic catalysis verification

Parameter	Value	Units
M_{tot}	60	mM
M as M_{red}	100	%
Y_{tot}	5	mM
Y as Y_{ox}	100	%
P_{tot}	6	μM
k_{M}^{0}	1	$\mathrm{cm\,s^{-1}}$
α_{M}	0.50	Dimensionless
k_{MP}	1×10^{8}	$\mathrm{M^{-1}\,s^{-1}}$
k_{cat}	1000	$\mathrm{s^{-1}}$
E_{M}^{0}	0.400	V
z_{M}	1	Dimensionless
z_{Y}	1	Dimensionless
D_{M}	5e-9	$\mathrm{cm^2\,s^{-1}}$
D_{Y}	6e-6	$\mathrm{cm^2\,s^{-1}}$
K_{M}	100	μM
l_1	5	μm
ζ_{x}	0.001	Dimensionless
d_{el}	2	mm
E	0.200	V
t_{eq}	500	s
t_{exp}	500	s
t_{rec}	500	s
T	20	°C
Space Points	2000	Dimensionless
Time Steps	1000	Dimensionless
β_1	0.01	Dimensionless
β_2	0.01	Dimensionless
Abs Tol	1×10^{-6}	Dimensionless
Rel Tol	1×10^{-4}	Dimensionless

6.2.2 Bimolecular Reaction

Successful implementation of the bimolecular catalysis portion of the model was verified by reduction of the reaction scheme such that it includes only the reaction of the mediator (which acts as a catalyst in this case) and electron acceptor Y with bimolecular kinetics. As in the enzymatic reaction verification, selection of a very small value of ζ_x (0.001), suitable dimensional parameters, and by setting SC1 and SC2 to zero, the model reduced to the "S" case of a reference model[4]. The obtained current-time curve is shown in figure 7A, and the concentration profile at a time of 1500 s is shown in figure 7B.

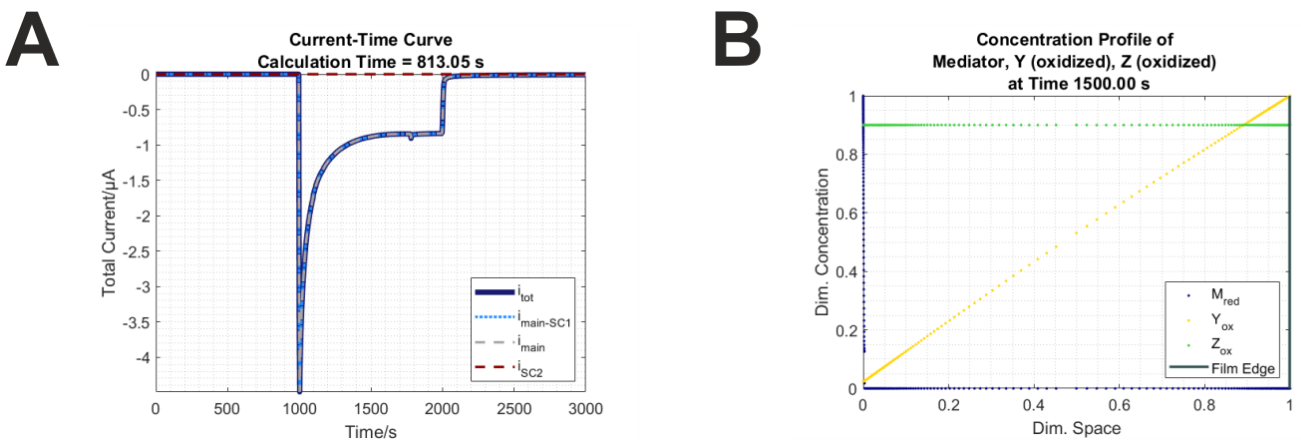

Fig. 7 Bimolecular catalysis section verification. Plots for the "S" case with fast rotation and no SC1: (A) Current-time curve, and (B) steady state concentration profile at 1500 s.

The analytical expression for prediction of the steady state current for a region S film (Table 2 in the reference article[4]) used for comparison is shown in equation 65. The calculated value ($-0.85\,\mu$A) is a close match to the obtained simulation result. The concentration profile matches what is expected for the S case, in which the mediator concentration sharply drops to zero near the electrode surface, and in which the electron acceptor Y concentration profile is linear within the film, reaching a value of zero close to the electrode surface. The simulation parameters are summarized in table 10.

$$i_{\mathrm{S}} = \frac{z_{\mathrm{M}} F A Y_{\mathrm{tot}} D_{\mathrm{Y}}}{l_1} \tag{65}$$

Table 10 Summary of parameters for bimolecular catalysis verification

Parameter	Value	Units
M_{tot}	5	mM
M as M_{red}	100	%
Y_{tot}	40	mM
Y as Y_{ox}	100	%
P_{tot}	1000	μM
k_M^0	1	$cm\,s^{-1}$
α_M	0.50	Dimensionless
k_{MP}	1×10^8	$M^{-1}\,s^{-1}$
k_{PY}	1×10^4	$M^{-1}\,s^{-1}$
E_M^0	0.400	V
z_M	1	Dimensionless
z_Y	1	Dimensionless
D_M	1×10^{-9}	$cm^2\,s^{-1}$
D_Y	7×10^{-8}	$cm^2\,s^{-1}$
l_1	100	μm
ζ_x	0.001	Dimensionless
d_{el}	2	mm
E	0.200	V
t_{eq}	1000	s
t_{exp}	1000	s
t_{rec}	1000	s
T	20	°C
Space Points	1000	Dimensionless
Time Steps	1000	Dimensionless
β_1	0.05	Dimensionless
β_2	0.01	Dimensionless
Abs Tol	1×10^{-6}	Dimensionless
Rel Tol	1×10^{-4}	Dimensionless

6.3 Solar Fuel Production Section Verification

Successful implementation of the solar fuel production portion of the model was performed by reduction of the overall process to match conditions in a reference model[4]. The parameters for the bimolecular reaction for solar fuel production were set with the purpose of once again recreating the "S" case, except with reaction between the mediator M and electron acceptor Z.

In the reaction scheme, either a bimolecular or an enzymatic reaction process is in between the electron transfer of the mediator and the reaction for the production of the solar fuel. For the case of enzymatic reaction, a combination of a high k_{cat} and low values of K_M and D_Y will cause the intermediate reaction process to have no impact on the overall kinetics, allowing for the system to be treated as the direct reaction between M and Z.

The resulting current-time curve, shown in figure 8A, and the concentration profile, shown in figure 8B, once again correspond to the "S" case, except that in this case, the Z_{ox} concentration profile linearly decreases within the film. The Y_{ox} concentration profile is at a constant value of 1 throughout the entire system, indicating that the selected parameter values were successfully set such that the intermediate reaction between P and Y posed no limitation to the overall kinetics.

The analytical expression for prediction of the steady state current for a region S film (Table 2 in the reference article[4]) used for comparison is shown in equation 66. The calculated value from the analytical expression ($-0.85\,\mu$A) closely matches the obtained simulation result ($-0.86\,\mu$A). The dimensional parameters used are summarized in table 11.

$$i_S = \frac{z_M F A Z_{tot} D_Z}{l_1} \tag{66}$$

6.3.1 Current-Time Curve and Concentration Profiles

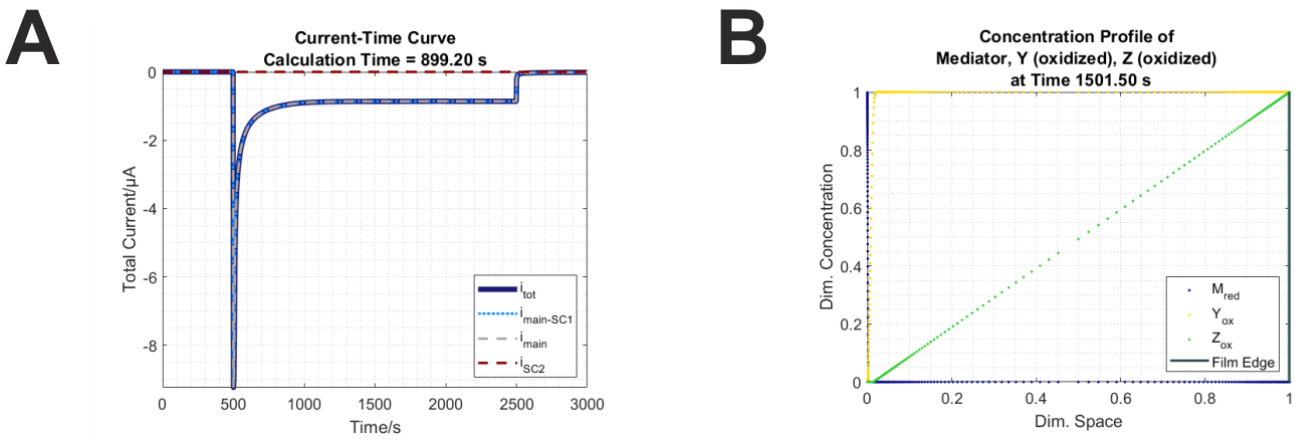

Fig. 8 Solar fuel section verification. Current time curve (A), and steady state concentration profile at 1501.5 seconds (B).

6.3.2 Summary of Parameters

Table 11 Summary of parameters for solar fuel production section verification

Parameter	Value	Units
M_{tot}	5	mM
M as M_{red}	100	%
Y_{tot}	5	mM
Y as Y_{ox}	100	%
Z_{tot}	40	mM
Z as Z_{ox}	100	%
P_{tot}	2000	μM
k_{M}^{0}	0.001	$\text{cm}\,\text{s}^{-1}$
α_{M}	0.50	Dimensionless
k_{MP}	1×10^{8}	$\text{M}^{-1}\,\text{s}^{-1}$
k_{PY}	1×10^{5}	$\text{M}^{-1}\,\text{s}^{-1}$
E_{M}^{0}	0.400	V
z_{M}	1	Dimensionless
z_{Y}	1	Dimensionless
D_{M}	1e-9	$\text{cm}^2\,\text{s}^{-1}$
D_{Y}	7e-9	$\text{cm}^2\,\text{s}^{-1}$
D_{Z}	7e-8	$\text{cm}^2\,\text{s}^{-1}$
l_{l}	100	μm
ζ_{x}	0.001	Dimensionless
d_{el}	2	mm
E_{hold}	0.200	V
t_{eq}	2000	s
t_{exp}	500	s
t_{rec}	500	s
T	20	°C
Space Points	1000	Dimensionless
Time Steps	1000	Dimensionless
β_1	0.05	Dimensionless
β_2	0.01	Dimensionless
Abs Tol	1×10^{-6}	Dimensionless
Rel Tol	1×10^{-4}	Dimensionless

6.4 Current Loss by SC1 Within the Film

6.4.1 Current-Time Curve and Concentration Profile When SC1 is Introduced

The current-time curves and static concentration profiles in the absence and in the presence of SC1 are shown in Figure 9. The parameters used for the simulations are given in table 12.

The current-time curve without SC1, shown in Figure 9A, showed a steady decay in current after initial illumination of the film, as is expected for stationary conditions. Also as expected, the total current decreased upon the introduction of SC1, as shown in Figure 9C; the loss of catalytic current due to SC1 can be seen by comparison of the calculated curves for the absence of SC1 (dotted light blue curve), and for the presence of SC1 (dashed grey line).

Inspection of the corresponding concentration profiles at 1501.5 s, shown in Figure 9B and Figure 9D, show two important qualitative features. Firstly, in contrast to the condition for no SC1 shown in Figure 9B, in which Y_{ox} is completely depleted at the electrode surface, the generation of Y_{ox} at the electrode surface due to SC1 causes its concentration at the electrode to increase above zero, as shown in Figure 9B. Secondly, in the presence of SC1, there is also a substantial change in the location of catalysis within the film. Inspection of the concentration profiles in the absence of SC1 (Figure 9B), shows that catalysis is limited to a narrow section near the electrode surface, because both of the reaction species (M_{red} and Y_{ox}) are present only very close to the electrode surface. In contrast, in the presence of SC1 (Figure 9D), significant concentrations of both reaction species are present throughout the entire film; therefore, catalysis within the film is decentralized in the presence of SC1.

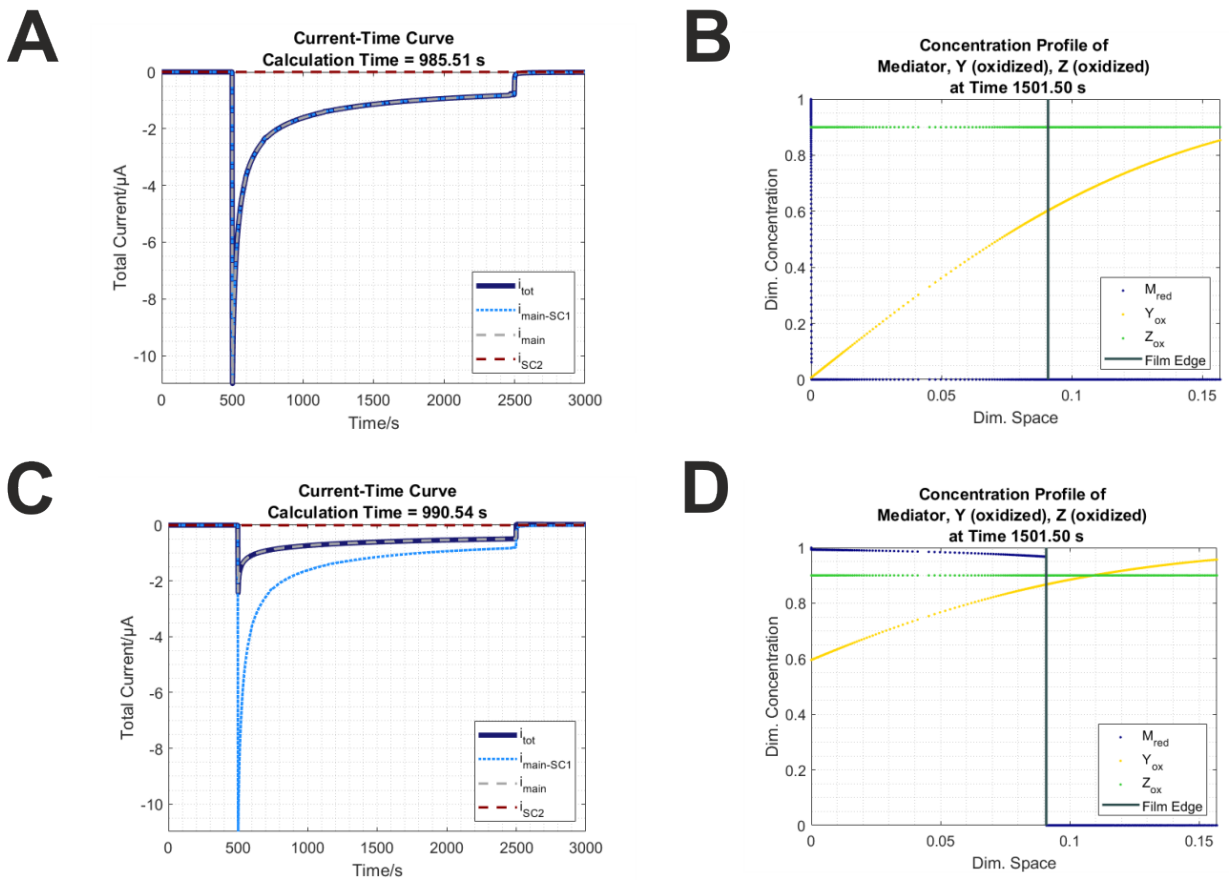

Fig. 9 Verification of the SC1 recombination portion of the model, based on calculated current-time curves for the case of the film (A) without SC1, and (C) with SC1, and on calculated concentration profiles at 1501.5 s for the case of the film (B) without SC1, and (D) with SC1.

6.4.2 Material Balance

Since the SC1 process involves the loss of a product that is firstly generated in a reaction, it does not conveniently collapse to a reference model as in the other cases. Therefore, a material balance, which takes into consideration the current-time curves and concentration profiles, was calculated for the quantitative verification of this part of the process. For the overall material balance, it is necessary to calculate the amount of Y_{red} produced and compare it with the amount of M_{red} reacted.

The equation used to calculate the amount of Y_{red} produced is shown in equation 67. Since Y_{ox} reacts to form Y_{red}, the amount of Y_{red} produced is equal to the decrease in the amount of Y_{ox}, when the initial and final amounts of Y_{ox} are compared. As indicated in the integral terms of equation 67, the beginning and ending dimensionless concentration profiles for Y_{ox} are separately integrated and compared to calculate the fraction of Y_{ox} that reacted. The collection of terms on the left side of equation 67 convert the dimensionless concentration to dimensional amount, using the initial total concentration of Y_{ox}, the percentage that was initially in the oxidized form, and the dimensions of the entire system (film and surrounding solution). For the collection of dimensional parameters listed in table 12, the amount of Y_{red} produced was 4.02 nmol.

$$(Y_{red})_{Produced} = Y_{tot}\,(\%\,as\,Y_{ox})\,A\,l_1\,(1+\zeta_x)\left[1-\frac{\int_0^1 (Y_{ox})_{t=1}\,dx}{\int_0^1 (Y_{ox})_{t=0}\,dx}\right] \tag{67}$$

M_{red} is replenished at the electrode surface as it is reacted for the production of Y_{red}. Therefore, the amount of M_{red} replenished at the electrode can be calculated by integration of the dimensionless current-time curve, shown in equation 68, where the factor on the left side containing n_M and F converts the dimensionless current to the amount of M_{red} replenished.

$$(M_{red})_{Electrode} = \frac{1}{z_M F}\int_0^1 \iota_{main}\,dt \tag{68}$$

Since the film initially contains M_{red}, then M_{red} from the film (which is not replenished at the electrode) can also contribute to the production of Y_{red}. As shown in equation 69, this quantity can be calculated by comparing the amounts of M_{red} in the film at the initial and final times by integration of the dimensionless concentration profiles. A conversion factor containing the initial total concentration, percentage that was M_{red}, and the film dimensions, converts the dimensionless concentration to the amount of M_{red}.

$$(M_{red})_{Film} = M_{tot}\,(\%\,as\,M_{red})\,A\,l_1\left[1-\frac{\int_0^1 (M_{red})_{t=1}\,dx}{\int_0^1 (M_{red})_{t=0}\,dx}\right] \tag{69}$$

The total amount of M_{red} reacted is then calculated by the addition of the contributions from replenishment at the electrode and from the film, as shown in equation 70. For the collection of dimensionless parameters listed in table 12, the total amount of M_{red} reacted was 8.04 nmol.

$$(M_{red})_{Reacted} = (M_{red})_{Electrode} + (M_{red})_{Film} \tag{70}$$

In the final step, the ratio of Y_{red} produced to M_{red} reacted was taken and was found to be 0.5004. Since z_M is equal to 1 and z_Y is equal to 2, the obtained value is in agreement with the value expected value of 0.5000 based on the reaction stoichiometry.

6.4.3 Summary of Parameters

Table 12 Summary of parameters for SC1 verification

Parameter	Value	Units
M_{tot}	5	mM
M as M_{red}	100	%
Y_{tot}	40	mM
P_{tot}	2500	μM
Y as Y_{ox}	100	%
k_{M}^{0}	1	$\mathrm{cm\,s^{-1}}$
α_{M}	0.50	Dimensionless
k_{MP}	1×10^{8}	$\mathrm{M^{-1}\,s^{-1}}$
k_{PY}	1×10^{4}	$\mathrm{M^{-1}\,s^{-1}}$
k_{SC1}	0 or 1×10^{6}	$\mathrm{M^{-1}\,s^{-1}}$
E_{M}^{0}	0.400	V
z_{M}	1	Dimensionless
z_{Y}	2	Dimensionless
D_{M}	1×10^{-9}	$\mathrm{cm^{2}\,s^{-1}}$
D_{Y}	7×10^{-8}	$\mathrm{cm^{2}\,s^{-1}}$
l_{1}	100	μm
ζ_{x}	10	Dimensionless
d_{el}	2	mm
E	0.200	V
t_{eq}	2000	s
t_{exp}	500	s
t_{rec}	500	s
T	20	°C
Space Points	1000	Dimensionless
Time Steps	1000	Dimensionless
β_{1}	0.05	Dimensionless
β_{2}	0.01	Dimensionless
Abs Tol	1×10^{-6}	Dimensionless
Rel Tol	1×10^{-4}	Dimensionless

7 Summary of Parameters for Charge Carrier Diffusion Coefficient Study

Table 13 Summary of parameters for charge carrier diffusion coefficient study

Parameter	Value	Units
M_{tot}	60	mM
M as M_{red}	100	%
Y_{tot}	5	mM
Y as Y_{ox}	100	%
P_{tot}	6	μM
k_M^0	0.01	$cm\,s^{-1}$
α_M	0.50	Dimensionless
k_{MP}	1×10^8	$M^{-1}\,s^{-1}$
k_{cat}	1000	s^{-1}
k_{SC1}	Variable	$M^{-1}\,s^{-1}$
E_M^0	0.600	V
z_M	1	Dimensionless
E_Y^0	0.276	V
z_Y	2	Dimensionless
D_M	5×10^{-9}	$cm^2\,s^{-1}$
D_Y	Variable	$cm^2\,s^{-1}$
K_M	100	μM
l_1	0.1	μm
ζ_x	100000	Dimensionless
d_{el}	2	mm
E	0.400	V
t_{eq}	20	s
t_{exp}	20	s
t_{rec}	20	s
T	25	°C
Space Points	1000	Dimensionless
Time Steps	1000	Dimensionless
β_1	0.02	Dimensionless
β_2	0.02	Dimensionless
Abs Tol	1×10^{-9}	Dimensionless
Rel Tol	1×10^{-7}	Dimensionless

References

1 M. E. Davis, *Numerical Methods and Modeling for Chemical Engineers*, Wiley, New York and Chichester, 1984.

2 A. J. Bard and L. R. Faulkner, *Electrochemical Methods: Fundamentals and Applications*, Wiley, New York, 2nd edn., 2001.

3 P. N. Bartlett and K. Pratt, *J. Electroanal. Chem.*, 1995, **397**, 61–78.

4 C. P. Andrieux, J. M. Dumas-Bouchiat and J. M. Savéant, *J. Electroanal. Chem. Interfacial Electrochem.*, 1982, **131**, 1–35.